The invasive and destructive behavior of HIV-induced T cell syncytia on collagen and endothelium

Andrew Sylwester, Karla Daniels, and David R. Soll
Department of Biological Sciences, The University of Iowa, Iowa City

Abstract: HIV-induced syncytia of the CD4$^+$ SUP-T1 T cell line mimic the subcellular organization of single cells and are able to crawl like single cells through extension of giant pseudopods. Because syncytia have been demonstrated in lymphoid tissue of HIV-positive individuals, their behavior has been investigated on more natural substrata, including dehydrated collagen, hydrated collagen, endothelial monolayers, and endothelial monolayers grown on collagen cushions. On hydrated collagen gels, both individual SUPT1 cells and syncytia form unusually long cylindrical projections that possess pseudopodial ends and are highly dynamic. Syncytia penetrate collagen gels through extension of these projections and disrupt their integrity. When incubated on endothelium, both single cells and syncytia readily traverse the monolayer through holes, and when incubated on endothelium supported by a collagen cushion, syncytia generate large holes through the monolayer, penetrate the monolayer, and disrupt the collagen gel through extension of long, complex projections. Invading syncytia also release viruses in a polarized fashion which adhere to and are taken up in vesicles by the endothelium. It is suggested that the destructive behaviors of syncytia which have been demonstrated in vitro may have correlates in vivo. *J. Leukoc. Biol.* 63: 233–244; 1998.

Key Words: *SUP-T1 · pseudopods*

INTRODUCTION

The human immunodeficiency virus (HIV) enters a CD4$^+$ T cell through an initial interaction between the virally encoded *env* protein gp120 and the CD4 receptor, and this interaction is facilitated by co-receptors [1]. Once a cell is infected, it expresses virally encoded gp120, a glycoprotein that is inserted into the plasma membrane of the host cell. The gp120 in the infected host cell membrane now can interact with the CD4 receptor of an uninfected T cell, resulting in cell fusion [2–5] and the genesis, after several rounds of fusion, of very large syncytia. In the past, syncytia have been observed in vivo primarily in the central nervous system of HIV-infected individuals, but recent results demonstrate that syncytia can and do form in lymphoid organs of HIV-infected individuals [6, 7], and for that reason must be considered as one possible avenue of T cell death in the progression of HIV-based disease.

Because syncytia are multinucleated and short-lived, it was initially assumed that they were disorganized fusion sinks in the throes of death and it was further assumed that they were not even the major pathway for T cell death in culture [8, 9]. However, recent results demonstrate that in infected cell cultures, syncytia are self-perpetuating and can be the major cause of T cell death [10]. More surprisingly, syncytia have been demonstrated to mimic the organization and behavior of single cells [11]. They are able to reorganize nuclei, cytoskeleton, endoplasmic reticulum, golgi, and mitochondria in order to mimic the subcellular organization of a single cell, and by the extension of giant pseudopods containing filamentous actin, they are able to establish cellular polarity and crawl with velocities, directionality, and a behavior cycle similar to that of a single cell [12–15, and D. Shutt, A. Sylwester, J. T. Stapleton et al., unpublished observations]. This is true not only for small syncytia, but also for syncytia that are several hundred times the volume of a single cell [12]. The possible repercussions of such behavior in vivo are twofold. First, because syncytia represent major sources of virus production, at least in culture [10], their capacity to migrate could result in viral dissemination throughout the human body. Second, because of their size and especially that of their pseudopods, their motile behavior could lead to serious disorganization and destruction of extracellular matrix and tissue. To begin to investigate the latter of these two possibilities, we have examined the motile behavior and the destructive effects of HIV-induced syncytia on collagen gels and endothelial monolayers in vitro.

MATERIALS AND METHODS

Virus, cells, and infection

HIV-1 IIIB virus originally isolated from a MOLT-3 human CD4$^+$ T cell line [16] was kindly provided by Dr. Ronald Kennedy of the University of Oklahoma

---

Abbreviations: PBS, phosphate-buffered saline; DMEM, Dulbecco's modified Eagle's medium; HIV, human immunodeficiency virus; FITC, fluorescein isothiocyanate; BSA, bovine serum albumin; SEM, scanning electron microscopy; TEM, transmission electron microscopy.

Correspondence: Dr. David R. Soll, Department of Biological Sciences, University of Iowa, Room 440, Iowa City, IA 52442. E-mail: drs@biovax.biol.uiowa.edu

Present address of Andrew Sylwester: National Institutes of Health, 9000 Rockville Pike, Bethesda, MD 20892.

Received May 16, 1997; revised August 21, 1997; accepted September 30, 1997.

Medical Center, Tulsa, OK. One-milliliter aliquots of infected MOLT-3 culture supernatant contained approximately 5000 tissue culture infectious dose 50 (5000 $TCID_{50}$).

SUP-T1 cells [17] were maintained in RPMI 1640 medium (Fisher Scientific, Pittsburgh, PA) supplemented with 10% heat-inactivated fetal calf serum, a 1:100 dilution of minimum essential medium nonessential amino acid solution (Sigma Chemical Co., St. Louis, MO), 10 mM *N*-2-hydroxyethylpiperazine-*N*′-2-ethanesulfonic acid, 1 mM sodium pyruvate, 2 mM L-glutamine, 100 units/mL penicillin, and 100 μg/mL streptomycin sulfate (referred to as supplemented RPMI medium). For infection, SUP-T1 cells were grown to 10^6 cells/mL in supplemented RPMI medium, pelleted, and 10^7 cells resuspended in 1 mL of supernatant from an HIV-1 IIIB-infected MOLT-3 culture. The mixture was incubated 2 h and then diluted with 9 mL of fresh supplemented RPMI medium. Parallel mock infections were performed, with 1 mL of supplemented RPMI medium used in place of virus-containing supernatant. After 2 h of incubation, cells were resuspended, then dispersed into fresh supplemented RPMI medium in 35-mm Falcon plastic T/C dishes at a final volume of 3.5 mL. Dishes were seeded with cells to an initial density of 125 cells/mm^2 and maintained at 37°C in a humidified 5% CO_2 atmosphere. For the analysis of syncytia, cultures were incubated for 48–72 h.

Preparation of collagen and endothelial substrates

To prepare collagen substrates, a 1.5-mg/mL solution of rat tail collagen (Sigma) in 0.1 M acetic acid was mixed with one-tenth volume of 10× Dulbecco's minimum essential medium (DMEM; GIBCO-BRL, Grand Island, NY) containing 20 mg/mL sodium bicarbonate. This solution was cast as 0.25-mm-thick layers on poly-L-lysine-treated plastic Petri dishes. Hydrated collagen gels were allowed to set at 37°C in 5% CO_2 for 2 h, then rinsed with three changes of fresh medium. To generate dehydrated collagen, hydrated gels were rinsed thoroughly with sterile water, allowed to air-dry in a sterile hood, then equilibrated against fresh medium. Endothelium substrates were prepared from bovine aortic endothelial cells, which were generously provided by Dr. Alex Sandra, Department of Anatomy, University of Iowa. Endothelial cells were inoculated into 35-mm-diameter Falcon T/C Petri dishes containing 3.5 mL DMEM medium supplemented with 10% heat-inactivated fetal calf serum with or without a hydrated collagen gel covering the surface. Seven days after confluency, the endothelial monolayers were used as substrates. For translocation experiments, plastic, collagen, and endothelial substrates were first incubated in supplemented medium. SUP-T1 cells were then distributed onto the substrate at a density of 500 cells/mm^2 and incubated for 48 h before analysis.

Fluorescent staining

To stain F-actin, cultures were gently mixed and aliquots pipetted onto 12-mm-diameter round glass coverslips previously treated with a poly-L-lysine solution. Coverslips were incubated in 5% CO_2 at 37°C for 30 min to allow cells to settle. Preparations were fixed in 2% glutaraldehyde plus 0.5% Triton X-100 in supplemented RPMI medium at 4°C for 5 min. Preparations were then rinsed two times with supplemented RPMI medium, one time with a 1:1 solution of supplemented RPMI medium and phosphate-buffered saline (PBS), and three times with PBS. Autofluorescence was quenched by treating coverslips with 5 mg/mL of $NaBH_4$ in PBS for 15 min, followed by three rinses with PBS. Preparations were then stained with a solution of 10 units/mL of fluorescein isothiocyanate (FITC)-conjugated phalloidin (Molecular Probes) in PBS, rinsed three times with PBS, mounted onto microscope slides with Vectashield mounting medium (Vector Labs, Burlingham, CA), and refrigerated overnight.

To stain tubulin, culture samples were allowed to settle onto poly-L-lysine-coated coverslips and fixed according to the procedures used for F-actin staining. Preparations were blocked for 1 h at 4°C with PBS plus 5% bovine serum albumin (BSA) and then exposed to 25 μL of undiluted anti-tubulin monoclonal antibody E7 obtained from the Developmental Studies Hybridoma Bank at The University of Iowa. Coverslips were rinsed three times in PBS containing 5% BSA and 0.02% NaN_3. After the final rinse, coverslips were incubated for 20 min at room temperature in 25 μL of FITC-conjugated goat $F(ab')_2$ fragment to mouse IgG (Cappel Research Products, Durham, NC) diluted 1:200 in PBS plus 5% BSA. Coverslips were rinsed two times in PBS plus 5% BSA, once in PBS, mounted in Vectashield mounting medium, and refrigerated overnight.

To stain endoplasmic reticulum, samples of live cultures were allowed to settle onto poly-L-lysine-coated coverslips and then stained with 0.25 μg/mL Rhodamine B hexyl ester R6 (Molecular Probes, Eugene, OR) in supplemented medium for 15 min in 5% CO_2 at 37°C. Preparations were rinsed twice with supplemented medium at 37°C, then fixed with 2% glutaraldehyde in supplemented medium for 5 min at room temperature. After two rinses with PBS, coverslips were inverted onto Vectashield on microscope slides.

Behavioral analyses

The methods used were similar to those previously described in detail [12, 13, 15]. In brief, cell cultures were positioned on the stage of a Zeiss Axiovert 100 inverted microscope equipped with a long distance condenser and a ×40 Plan objective with a numerical aperture value of 0.60. A temperature of 37 ± 1 °C was maintained by a thermostat-controlled air curtain or heated stage. Cell behaviors were video recorded at a single focal plane with a Newvicon 2400-07 video camera (Hamamatsu Photonics K.K., Japan). Cell images were frame-grabbed and manually digitized into the Dynamic Image Analysis System (DIAS) data base [18–20], based in a Macintosh Quadra computer (Apple Computers, Cupertino, CA). Instantaneous velocity was measured according to methods previously described in detail [18].

Scanning and transmission electron microscopy

For scanning electron microscopy (SEM), cells were prepared according to methods previously described [12] and imaged with a Hitachi-4000 scanning electron microscope. For transmission electron microscopy (TEM), cells were prepared according to methods previously described [21] and imaged with a Hitachi 7000 electron microscope.

RESULTS

The behavior of HIV-induced syncytia on collagen gels

A majority of SUP-T1 cells and syncytia form pseudopods on both dehydrated collagen, which is a lightly packed mesh of collagen fibers, and hydrated collagen, which is a loosely packed mesh of collagen fibers [15]. However, only approximately one-third to one-half of single cells actually translocate on either substrate, and while approximately half of syncytia translocate on dehydrated collagen, no syncytia translocate on hydrated collagen [15]. When scanning electron micrographs of cells incubated on dehydrated and hydrated collagen were examined, the majority in both cases were found to possess single, broad pseudopods (**Fig. 1a** and **Fig. 2a**), but a minority in each case possessed unusual elongate projections (Figs. 1b and 2b). On both dehydrated and hydrated collagen, these cylindrical projections grew to lengths as great as 80 μm and possessed pseudopod-like ends (e.g., p-l in Fig. 1b). Similar elongate processes were not observed in SEMs of cells incubated for similar periods on conditioned tissue culture plastic (data not shown), a substratum that supports cellular locomotion to approximately the same degree as dehydrated and hydrated collagen [15].

To obtain an accurate estimate of the proportion of SUP-T1 cells that formed these unusual projections, 777 individual cells on dehydrated collagen and 575 individual cells on hydrated collagen were video-recorded for periods of 3–8 min, and the videos scanned for the formation and behavior of elongate cylindrical processes. One percent of cells on dehydrated collagen and twelve percent of cells on hydrated

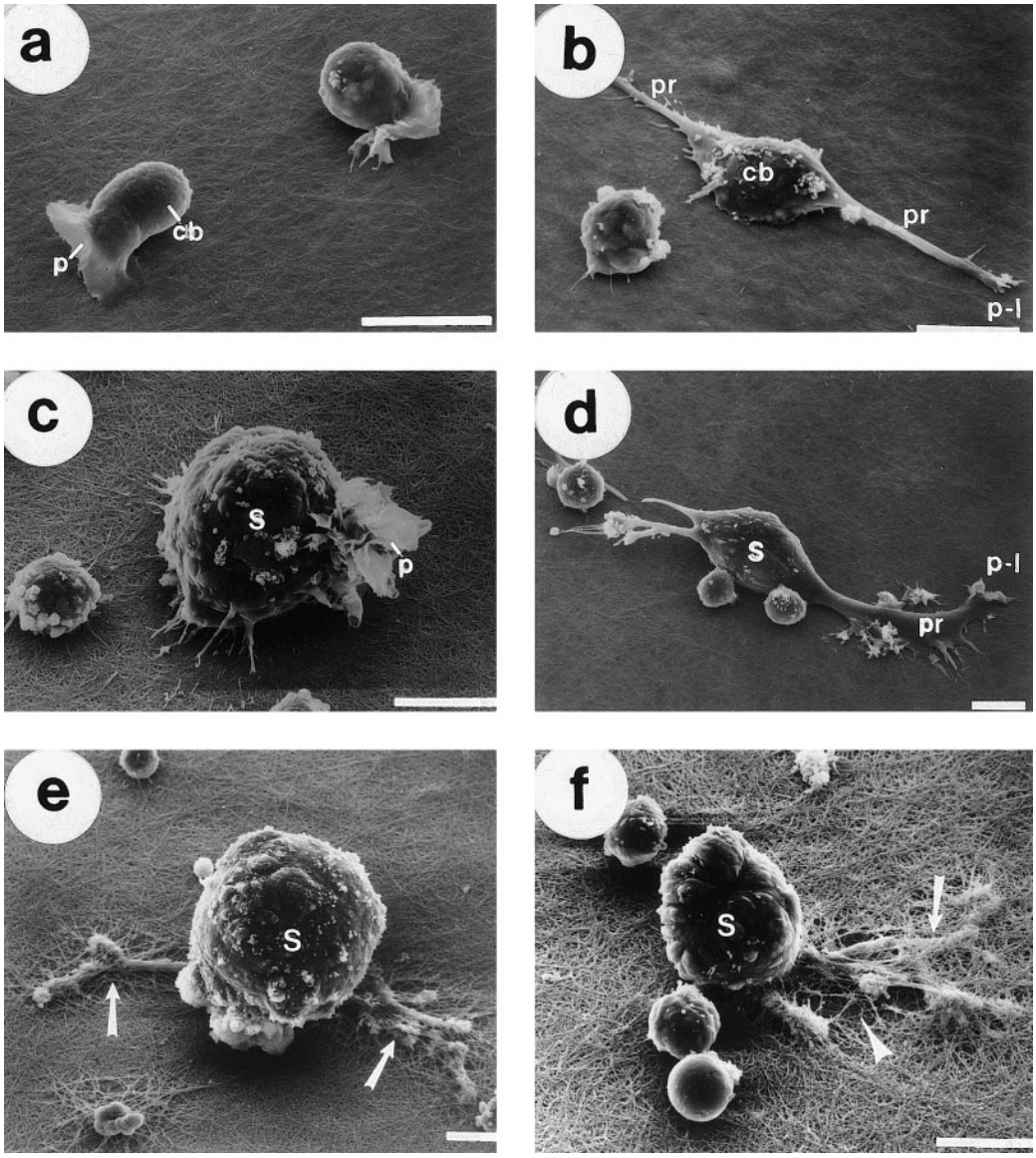

Fig. 1. Scanning electron micrographs of SUP-T1 cells and syncytia incubated on dehydrated collagen. (a) Two cells from an uninfected SUP-T1 culture exhibiting round cell bodies and broad ribbon-like pseudopods after 30-min incubation. (b) Cells from an infected culture, one of which is extending two elongate, cylindrical projections after 30-min incubation. (c) A syncytium with a round body and a broad ribbony pseudopod after 30-min incubation (note that the pseudopod is approximately 16× as large as the single cell to the left of the micrograph). (d) Syncytium extending multiple elongate cylindrical processes along the surface of the dehydrated collagen gel. (e, f) Syncytia extending multiple elongate processes that are disrupting the dehydrated collagen gel after 72-h incubation. cb, cell body; p, pseudopod; pr, cylindrical process; s, syncytium body; p-l, pseudopod-like terminus; arrows in panel e and f point to mutiple complex processes; arrowhead in panel f points to disrupted collagen mesh. Scale bars, 10 μm.

collagen formed elongate cylindrical processes. In all cases, the processes were dynamic. In **Figure 3**, **a** and **b**, sequential video frames are presented of elongate processes during an 8- and 10.5-min period, respectively. In both cases, changes in shape, length, and branching occurred during extension and retraction of the process.

When SEMs of HIV-induced SUP-T1 syncytia incubated on dehydrated collagen for 30 min were examined, the majority possessed single, blunt pseudopods (Fig. 1c), but a minority extended one or more cylindrical projections with pseudopodial ends (Fig. 1f). Video recordings of 36 syncytia were analyzed for periods of 3–8 min. Eight percent of syncytia were observed to form these projections. In all cases the projections were dynamic (date not shown), just as in the case of projections formed by single cells (Fig. 3). When syncytia were incubated for periods up to 72 h on dehydrated collagen, the projections penetrated the tight fiber mesh and disrupted its integrity (Fig. 1, e and f).

When SEMs of syncytia incubated on hydrated collagen for 30 min were examined, all were found to have formed elongate projections that penetrated the loose fiber matrix (data not shown). In a video analysis of 20 syncytia incubated on hydrated collagen, close to 60% were observed extending a cylindrical projection. This is considered an underestimate because many of the projections burrowed into the collagen matrix under the cell and were not visible in the videos. Again, all projections were dynamic (data not shown). When syncytia were incubated on hydrated collagen for 72 h or more, the

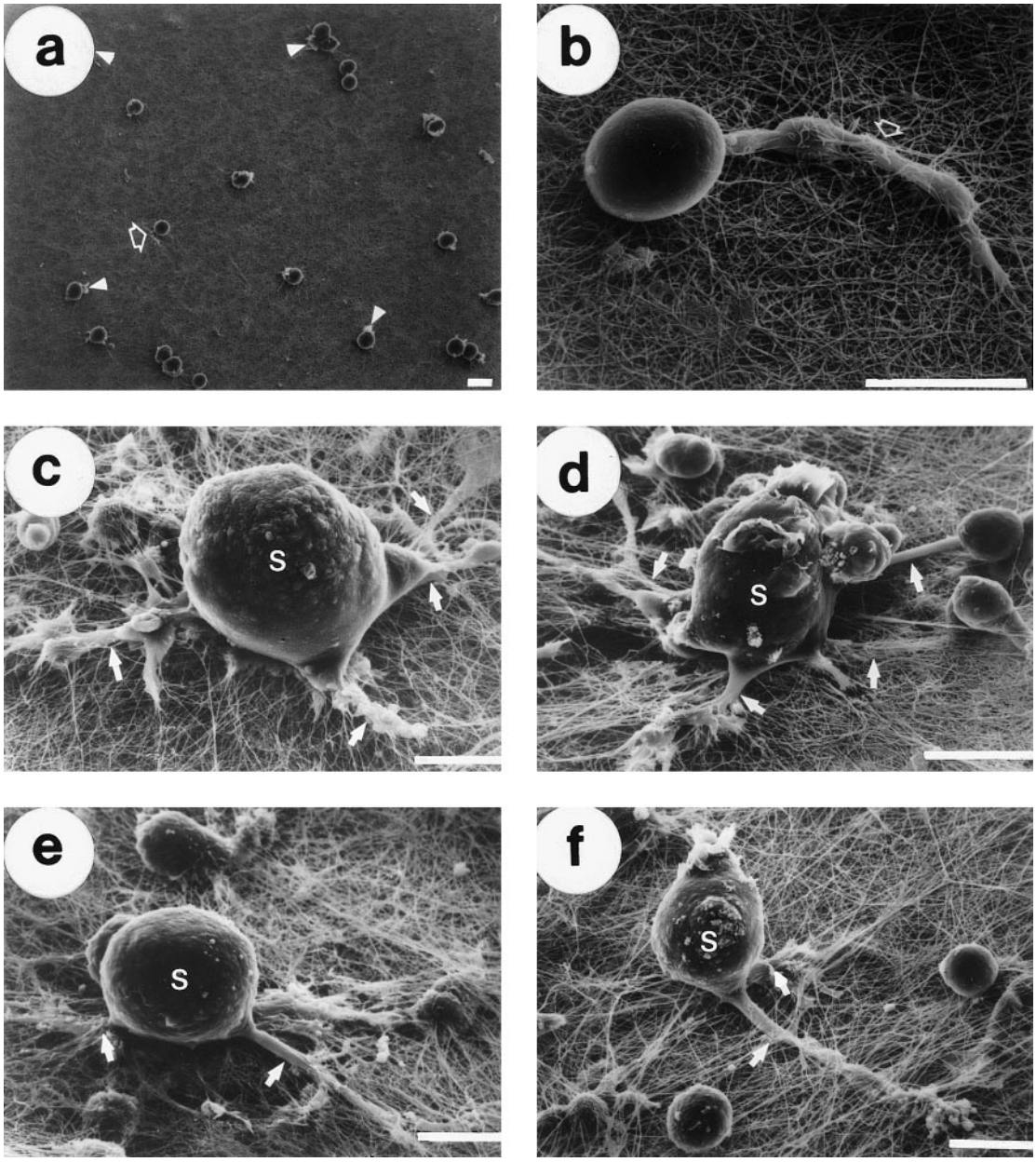

Fig. 2. Scanning electron micrographs of SUP-T1 cells and syncytia incubated on hydrated collagen. (a) Low magnification of single cells after 15-min incubation; most cells (arrowheads) are extending blunt, broad pseudopods, and one (unfilled arrow) is extending complex protrusions into the gel. (b) Higher magnification image of a cell that has extended an elongate process (unfilled arrow) into the gel. (c, d, e, f) Syncytia that have extended complex multiple processes that are penetrating and disrupting the collagen gel. S, syncytium. Unfilled blunt arrow in panel b and filled arrows in panels c, d, e, f point to elongate cylindrical or complex extensions. Scale bars, 10 μm.

majority of syncytia extended multiple projections into the matrix, and the matrix was severely disrupted (Fig. 2, c–f), presumably the result of the dynamic nature of the projections.

Cylindrical projections share cell body and pseudopod characteristics

Because elongate projections formed by both single cells and syncytia were dynamic, one might expect them to possess the subcellular organization of a pseudopod along their entire length. However, only the termini of the projections exhibited the ribbon-like morphology of blunt pseudopods. To determine the nature of projections, they were analyzed for components differentially localized in traditional pseudopods (F-actin) and in the main cell bodies of T cells (microtubules, endoplasmic reticulum, mitochondria) [12, 13, 21, 22]. The cortex as well as regions of microspikes and pseudopod-like termini of cylindrical projections from both single cells (**Fig. 4a**) and syncytia (Fig. 4b) stained differentially for F-actin, suggesting that they were pseudopod-like along their entire length. Cylindrical projections, however, also stained intensely for both endoplasmic reticulum (Fig. 4, c and d) and microtubules (Fig. 4e), suggesting that they shared characteristics with the main cell body. In electron micrographs, cylindrical projections were also demonstrated to contain mitochondria (data not shown), another

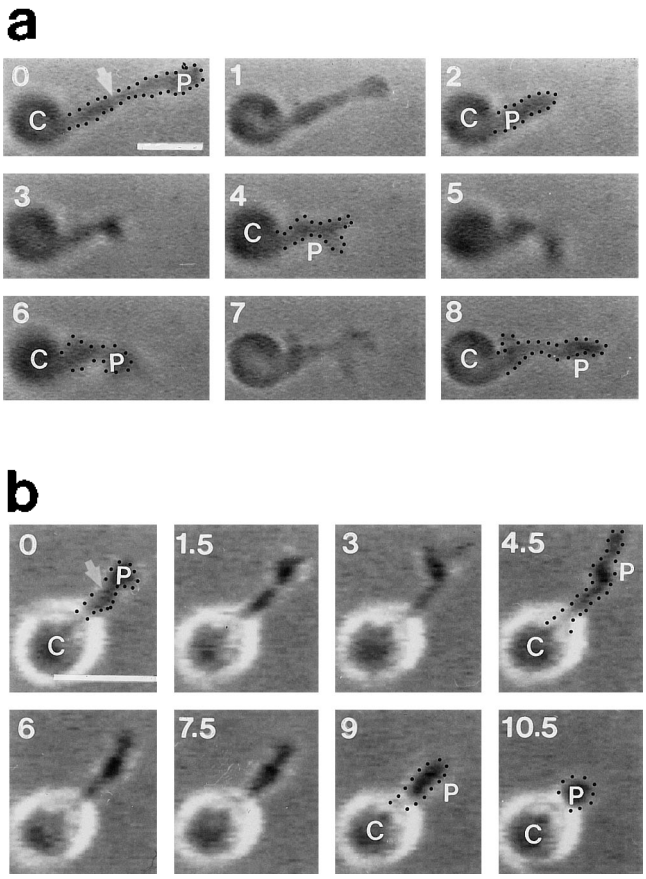

Fig. 3. Video sequences demonstrating the dynamic behavior of elongate processes extended by individual SUP-T1 cells in hydrated collagen. Because the collagen gel is opalescent, the still-frame video images do not provide high-contrast images of the projections. Therefore, the perimeters of projections have been interpreted from dynamic videos and outlined with black dots in intermittent frames. Time is presented in the upper left corner of each frame in minutes. (a) A cell after 48 h of incubation on hydrated collagen. (b) A cell after 6 h on hydrated collagen. C, cell body; P, cylindrical process. Scale bars, 10 μm.

cytoplasmic component usually excluded from the pseudopod. Together, these results suggest that cylindrical projections share characteristics of both the cell body and the pseudopod.

Syncytia penetrate endothelial monolayers supported by a collagen gel in a unique fashion

The proportion and velocity of motile cells and syncytia on bovine aortic endothelium (BAE) are both reduced when compared with cells incubated on conditioned tissue culture plastic or dehydrated collagen [15]. Video analysis demonstrated that both cells and syncytia incubated on BAE grown on plastic readily penetrated the monolayer, entering the endothelium-plastic interphase, and readily emerged from this space back through the monolayer (data not shown). Because of the opulescent nature of BAE monolayers, the dynamics of pseudopods and the possible formation of cylindrical or complex extensions were not readily assessable by conventional video analysis.

To assess the destructive behavior of HIV-induced syncytia on BAE, we analyzed cells and syncytia incubated on a model in which BAE was grown as a monolayer on a cushion of hydrated collagen. In SEMs, individual cells from infected cultures incubated for 48–72 h were found associated with small holes in the monolayer (**Fig. 5 a–c**). In most cases, the cell had extended a pseudopod (Fig. 5, a, b) or elongate cylindrical projection (Fig. 5c) through the hole. Similar results were obtained with syncytia incubated for 48–72 h on BAE monolayers, but the holes in the monolayer were far larger. In SEMs, the majority of syncytia were found associated with holes with diameters equal to or greater than that of the syncytium body (Fig. 5, d–f). In most cases, a pseudopod or a complex, elongate projection penetrated the collagen cushion exposed in the hole of the monolayer.

There are two alternative explanations for the association of holes with cells and syncytia. First, holes may appear spontaneously in endothelial sheets, and cells and syncytia may search them out in the process of invasion. Alternately, cells and syncytia may induce or generate such holes. BAE monolayers cultured in the absence of SUP-T1 cells or syncytia formed holes spontaneously, but the holes, although sometimes larger than those associated with single cell pseudopods and projections, were far smaller than those associated with syncytia. To test directly whether syncytia induce giant holes in BAE monolayers, isolated syncytia were individually seeded onto unperturbed BAE monolayers atop collagen gels and examined by SEM 12 h later. A representative experiment is presented in **Figure 6a** and **b**. The seeded syncytium was approximately 900 single cell volume-equivalents (CVE), and after 12 h sat within a hole greater than 200 μm in diameter. Nine pseudopod-tipped projections were visibly in contact with the underlying collagen cushion (Fig. 6a). In a low-magnification view, no other large holes were evident in the monolayer (Fig. 6b). It seems highly unlikely that in 12 h this single seeded syncytium would have searched for the single hole in the entire BAE monolayer. It is far more likely that the syncytium induced the hole. Additional syncytia with volumes of 370 and 420 single CVE were seeded on BAE monolayers, and the same result was obtained (Fig. 6, c and d, respectively). In each case, a large hole was associated with the syncytium, and no hole greater in diameter than 15 μm was observed in the monolayer within a 500-μm radius of the seeded syncytium.

In **Figure 7a**, a TEM is presented of a moderate-sized syncytium 2 h after it had been seeded onto a BAE monolayer. It had just begun to penetrate the monolayer through a hole equal in diameter to that of the pseudopod. The smooth edges of the hole in the endothelium were in contact with the penetrating pseudopod. The penetrating pseudopod had begun to spread under the monolayer onto the supporting collagen cushion. No viruses were observed budding from this syncytium. In Figure 7b, a TEM is presented of a moderate sized syncytium 6 h after it had been seeded onto a BAE monolayer. In contrast to the syncytium incubated for 2 h (Fig. 7a), the endothelial cell(s) had withdrawn and were not in contact with the penetrating portion of the syncytium (Fig. 7b). In this example, virus were actively budding in a polar fashion along the edge of the syncytium opposing the monolayer and mitochondria were localized in the portion of the syncytium penetrating the hole in the endothelium (Fig. 7b). In Fig. 7c, a TEM is presented of a

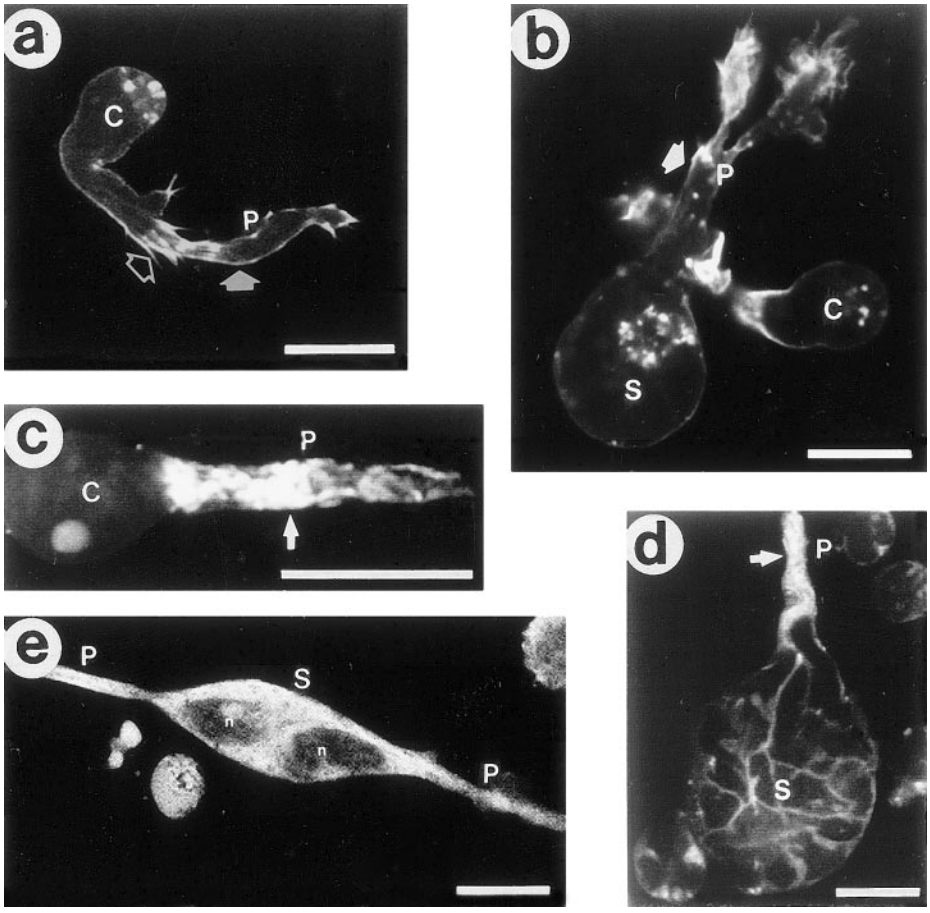

Fig. 4. The distribution of F-actin, endoplasmic reticulum, and tubulin in elongate cylindrical processes formed by cells and syncytia on hydrated collagen. (a) An uninfected cell incubated for 2 h then stained for F-actin (unfilled arrow, intense cortical staining at microspike region; filled arrow, moderate cortical staining). (b) A small syncytium and an individual cell incubated for 48 h and then stained for F-actin (filled arrow, intense staining in cylindrical projection). (c) An individual cell that has formed a cylindrical process, stained for endoplasmic reticulum. (d) A syncytium that has formed a cylindrical process, stained for endoplasmic reticulum (filled arrow, intense staining in projection). (e) A small syncytium stained for tubulin. C, cell body; S, syncytium body; P, protrusion; n, nucleus. Scale bars, 10 μm.

large syncytium 12 h after it had been seeded on a BAE monolayer. Again, it is clear that the endothelial cell is retracting and not in contact with the penetrating portion of the syncytium. In Figure 7d, an example is presented of a syncytium 12 h after seeding that had begun to engulf an endothelial cell.

In **Figure 8a**, a TEM is presented of a portion of a very large syncytium 96 h after it had been seeded on a BAE monolayer. Because of the size of this syncytium (90 μm in length, 200 CVE), it was photographed in sections and the photos assembled as a montage. The syncytium had generated a large hole 80 μm in diameter in the monolayer. The pseudopod of the syncytium had penetrated the underlying collagen cushion. The visible extension penetrating the cushion contained mitochondria (Fig. 8a), just as the penetrating extension of the syncytium in Figure 7b. The syncytium was in the act of releasing large numbers of virus in a polarized fashion from its surface adjacent to the hole and closest to the invading pseudopod (Fig. 8, a, b, c), just as the syncytium in Figure 7b. Virus was also attached to the BAE and membrane-bound in the BAE (Fig. 8d). Similar vesicles containing virus were observed in endothelial cells in additional montages.

DISCUSSION

T cells spend a major portion of their lives in tissue stroma [23] and, therefore, must continuously interact with both the extracellular matrix and the surfaces of surrounding cells. In addition, circulating T cells migrate through blood vessel walls to lymphoid organs and into inflamed tissues [24–27]. T cells infected with HIV can form large, multinucleated syncytia in vitro [2–5] and recent studies in vivo have demonstrated that in addition to the central nervous system [e.g., see refs. 28–30], such syncytia can be found in adenoid and tonsillar tissue [6, 7], as well as lymph node tissue [D. Shutt, A. Sylwester, J. T. Stapleton et al., unpublished observations]. In addition, it has been demonstrated that syncytia formed in vitro in both infected SUP-T1 cell cultures and peripheral blood T cell cultures are capable of mimicking the subcellular organization and polarity of single cells and, through extension of a giant pseudopod, are capable of translocating along the surface of a plastic tissue culture dish [12, 13, 15]. More importantly, it has been demonstrated that syncytia formed in the lymph nodes of HIV-positive individuals in vivo are motile [D. Shutt, A. Sylwester, J. T. Stapleton et al., unpublished observations]. If syncytia can form in vivo, and if they can be motile, how would they behave in tissue stroma and at the walls of blood vessels? To begin to answer this question, we have compared the morphology and behavior of individual SUP-T1 cells and HIV-induced T cell syncytia incubated on dehydrated and hydrated collagen gels, and on a vessel wall model of BAE grown to confluency on hydrated collagen. Collagen is a major component of the extracellular matrix [31], and collagen gels are physically and chemically similar to tissue stroma [32]. The BAE monolayer formed in vitro and its basal lamina exhibit the properties and molecular composition of in vivo vascular endothelium [33, 34], with closely apposed cells with tight

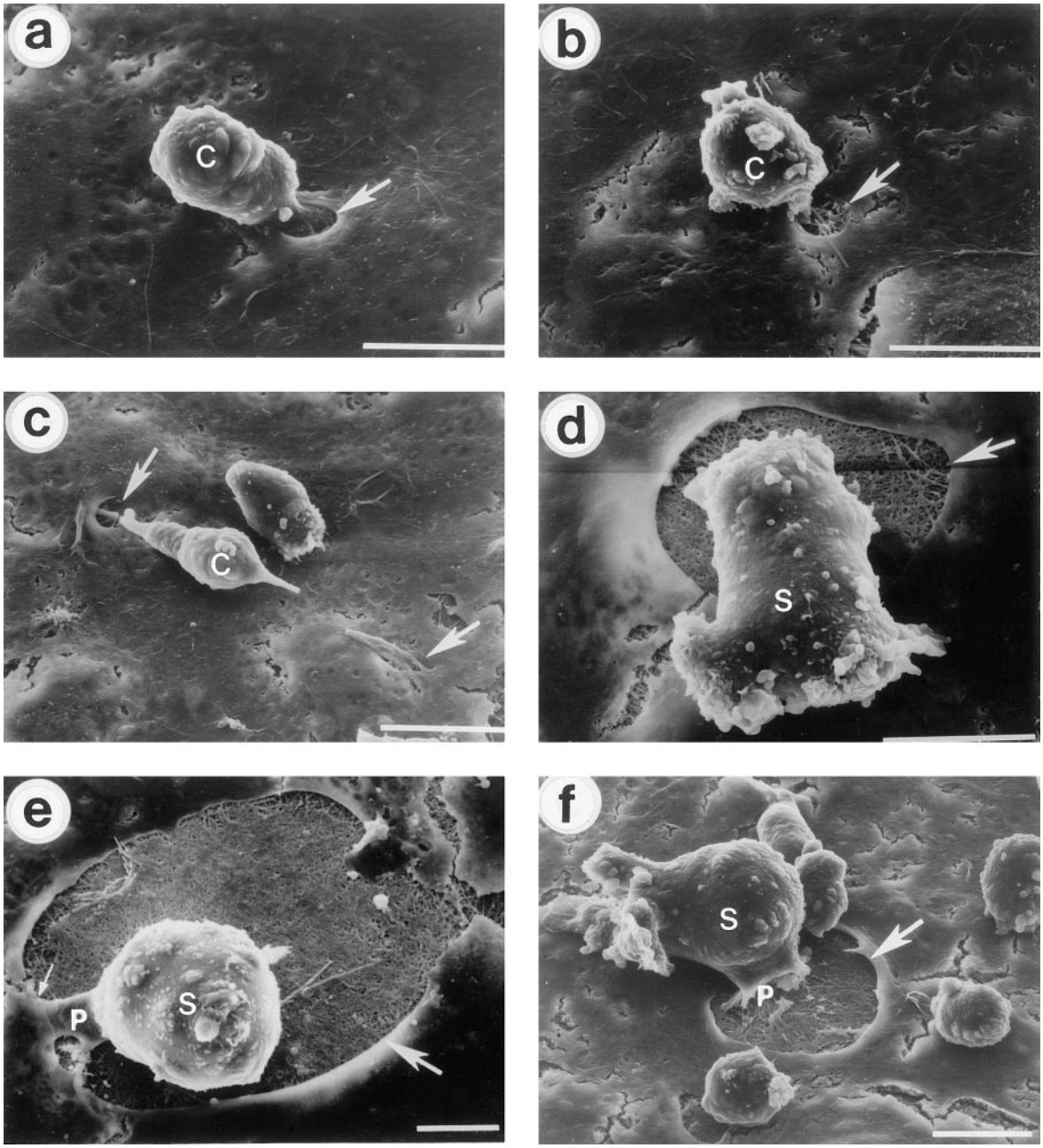

Fig. 5. Scanning electron micrographs of single cells and HIV-induced syncytia incubated on bovine aortic endothelial (BAE) monolayers grown to confluency on hydrated collagen cushions. (a, b) Individual cells from uninfected cultures penetrating small, smooth-edged holes in the monolayer (note that the collagen fibers in the supporting cushion are visible through the hole). (c) An uninfected cell penetrating two smooth-edged holes simultaneously in the monolayer through cylindrical protrusions. The right hand protrusion has been broken in preparation for SEM. (d, e, f) Syncytia penetrating the monolayer through very large smooth-edged holes in the monolayer. Arrows denote the edge of the holes. Scale bars, 10 μm.

junctions, and vectoral secretion of collagens, laminin, fibronectin, and dermatin sulfated proteoglycans [35–37]. Previous studies of lymphocyte motility and invasion have employed this model [38–40].

Behavior on collagen

Lymphocytes have been demonstrated to invade collagen gels [41, 42] and collagen has been demonstrated to enhance leukocyte motility [42, 43]. Lymphocytes have also been demonstrated to express a receptor for collagen [43–45], to adhere to collagen [43–46], and to disrupt and degrade collagen matrices [46–50]. Here, we have demonstrated that approximately half of the cells in a SUP-T1 population actively translocated across the surface of a dehydrated or hydrated collagen gel and that cells readily penetrated hydrated collagen gels. Approximately 1% of individual cells on dehydrated collagen and 12% on hydrated collagen formed unusual cylindrical extensions, which were dynamic but did not function as locomotary agents for cellular translocation (i.e., the cell bodies were relatively immobile). In hydrated collagen, these projections became entangled in collagen fibers, but the capacity to retract these projections indicated that they did not

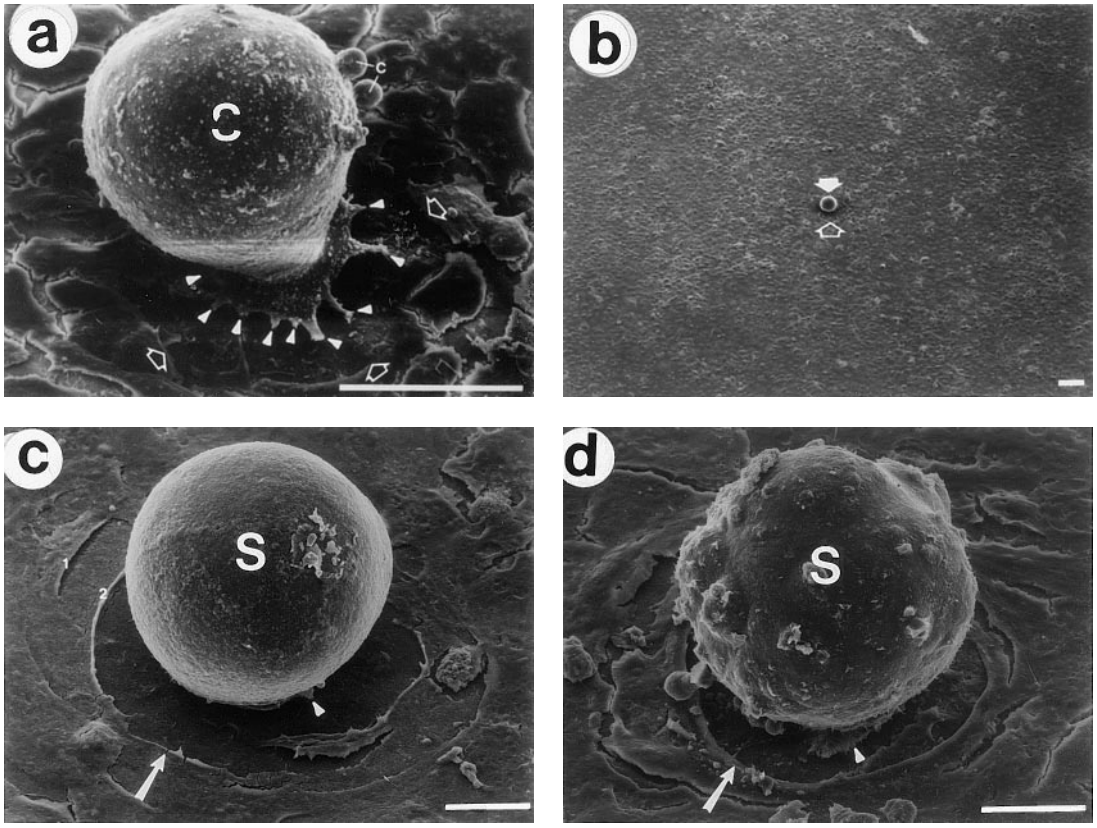

Fig. 6. Syncytia generate large holes in bovine aortic endothelial (BAE) monolayers. Scanning electron micrographs of individual syncytia 12 h after they were seeded onto monolayers grown to confluency atop a hydrated collagen cushion. (a, b) High and low magnification, respectively, of the same syncytium. Note that the only large hole in the endothelial monolayer is directly under the syncytium. Arrowheads in panel a point to projections emanating from the syncytium and attached to the collagen cushion. Filled arrow and unfilled arrow in panel b point to syncytium and edge of hole, respectively. Scale bars in panels a and b, 100 μm. (c, d) Two additional cases of individual syncytia 12 h after each had been seeded on a monolayer. Low magnification views (not shown) demonstrated in each case that there were no other holes with diameter greater than 20 μm in the endothelial monolayers within a 500-μm radius of the seeded syncytium. Scale bars in panels c and d, 20 μm.

become irreversibly attached to the collagen fibers in the matrix. Morphologically similar processes have been demonstrated emanating from lymphocytes incubated on collagen [46], from lymphoma cells incubated on endothelial basal lamina [51], and from $CD8^+$ T cells incubated on monolayers [52, 53], so these processes are not unique to the cell type and conditions employed in this study.

Syncytia also translocated on dehydrated collagen, but at significantly reduced frequency and average velocity [15]. Syncytia did not translocate on hydrated collagen [15]. SEM analysis demonstrated that the majority of syncytia on hydrated collagen had formed one or more complex projections that penetrated the collagen gel. It seems reasonable to suggest that the incapacity of syncytia to translocate on hydrated collagen is due to pseudopodial invasion of the gel. Long cytoplasmic processes have also been found emanating from multinucleated giant cells in autopsies of three AIDS patients who had suffered from encephalitis [30], demonstrating that syncytia can form these processes in vivo.

The complex processes that syncytia extended into hydrated collagen became entwined in the collagen mesh and disrupted the organization of the gel in their immediate vicinity. Video analyses of these projections demonstrated that they were mobile, continuously elongating or retracting, and continuously changing shape. The most active and morphologically plastic portion was their distal terminus, which in SEM analysis were found to have the same general shape as the broad, ribbon-like pseudopods emanating directly from cells and syncytia actively translocating on conditioned tissue culture plastic. The elongate, cylindrical projections formed by single cells and syncytia appeared to be superficially similar, but syncytia tended to form projections that, on hydrated collagen, were larger and exhibited more complex shapes.

The motile behavior of the cylindrical processes extended by syncytia on collagen gels must be, in part, the basis for the disorganization of the collagen gel in the immediate vicinity of the syncytia. Because cellular motility is for the most part accomplished through the highly regulated polymerization of actin in pseudopods [54], we were interested in assessing whether these were, in fact, simply highly elongated pseudopodia. The cortex of T cell pseudopods stain intensely for F-actin [12, 13, 22] and we found that at least portions of the cortex of the long cylindrical extensions also stained intensely, although the most intense staining was usually localized at the terminus of a projection. However, T cell pseudopods contain few microtubules and are usually devoid of endoplasmic reticulum and mitochondria [22], whereas elongate projections contained all three. These results suggest that the elongate cylindrical projections of single cells and syncytia formed on dehydrated

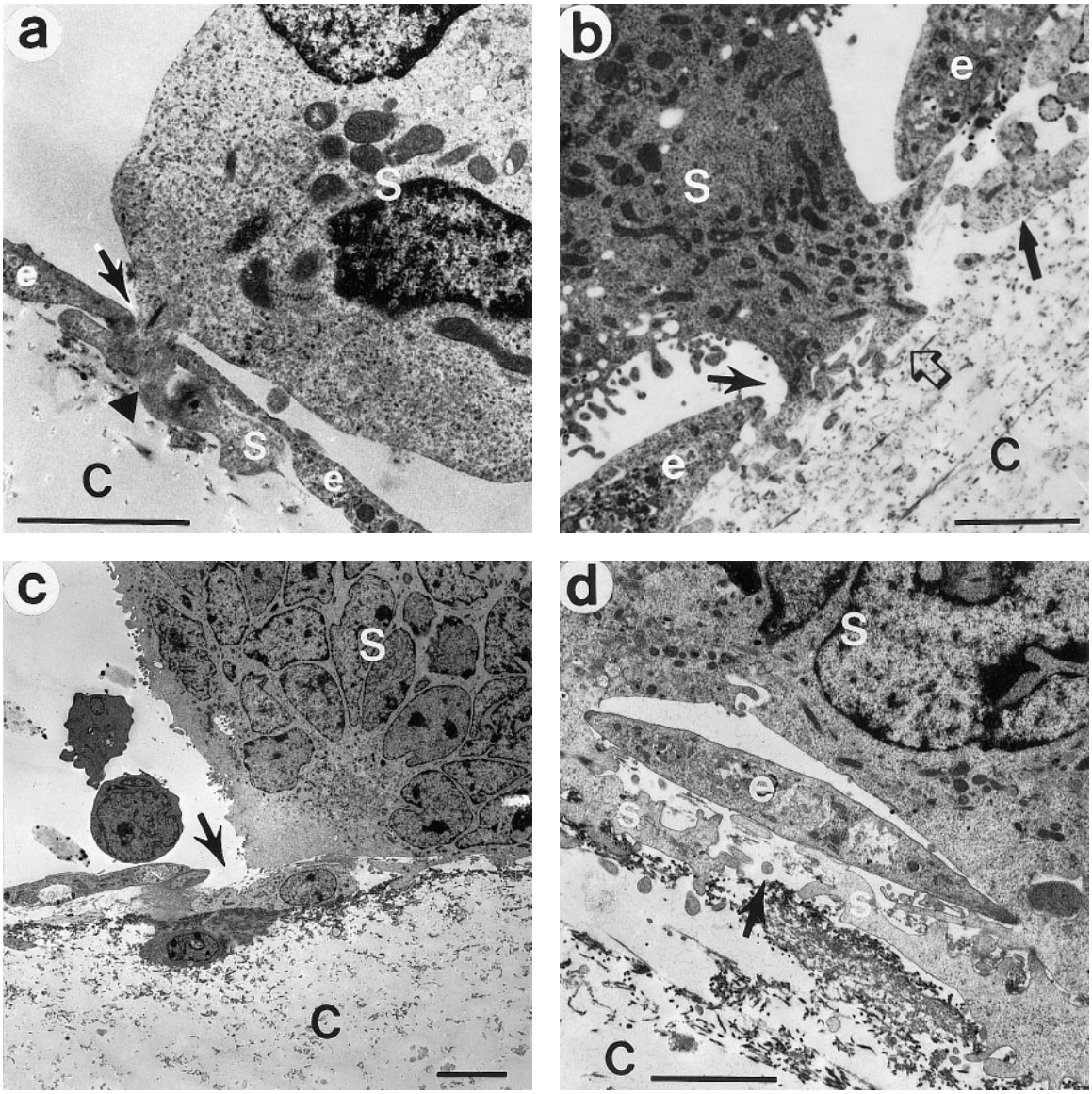

Fig. 7. Transmission electron micrographs of syncytia penetrating a bovine aortic endothelial (BAE) monolayer. (a) A small syncytium seeded on a monolayer and incubated for 2 h before fixation and processing for TEM. Note that the syncytium has penetrated the monolayer by extension of a cell projection (black arrowhead) that has expanded between the monolayer and collagen cushion, and that the edge of endothelial cells are in contact with neck of the syncytium extension. (b) A large syncytium seeded on a monolayer and incubated for 6 h before fixation and processing for TEM. Note that the endothelial cells are not in contact with the neck of the syncytium projection (narrow filled arrow points to space between neck of syncytium and endothelium; unfilled arrow points to projection; blunt filled arrow points to penetrating projection). (c) A very large syncytium after 12 h on monolayer (arrow points to space between syncytium and endothelium). (d) Example of syncytium engulfing an endothelial cell. S, syncytium; e, endothelial cell; C, collagen cushion. Scale bars, a, b, 3 μm; c, 10 μm; and d, 5 μm.

and hydrated collagen shared organizational characteristics of both the cell body and the traditional pseudopod.

Behavior on endothelium

The process of leukocyte migration from the luminal to abluminal side of vascular endothelium has been studied extensively in vitro and in vivo. In vivo steps in the process include rolling of homing receptor bearing leukocytes along cognate adhesion bearing endothelium, activation of leukocytes to a motile phenotype, development of firm attachments, invasion of the endothelium, passage through the basement membrane, and migration into tissue stroma [23, 24, 26, 27, 55–59]. Leukocytes appear to have different solutions for passage through endothelium. On monolayers with tight junctions, recent studies indicate that most lymphocytes pass through junctions, but some nonjunctional passage also occurs [47, 51, 60, 61]. Several studies suggest that holes form in the endothelium through endothelial cell retraction [47, 62].

SUP-T1 cells incubated on BAE monolayers can translocate along the surface of the monolayers, but at velocities lower than on conditioned plastic or collagen [15]. Cells readily penetrated these monolayers through smooth-edged holes not necessarily at endothelial cell-cell junctions. An SEM analysis of single cells on top of the monolayer demonstrated that in some cases single cells extended pseudopods or elongate cylindrical projections into the monolayer through small smooth-edged holes. Such behavior may result in an anchoring effect and may, therefore, be the basis for the depressed rates of translocation.

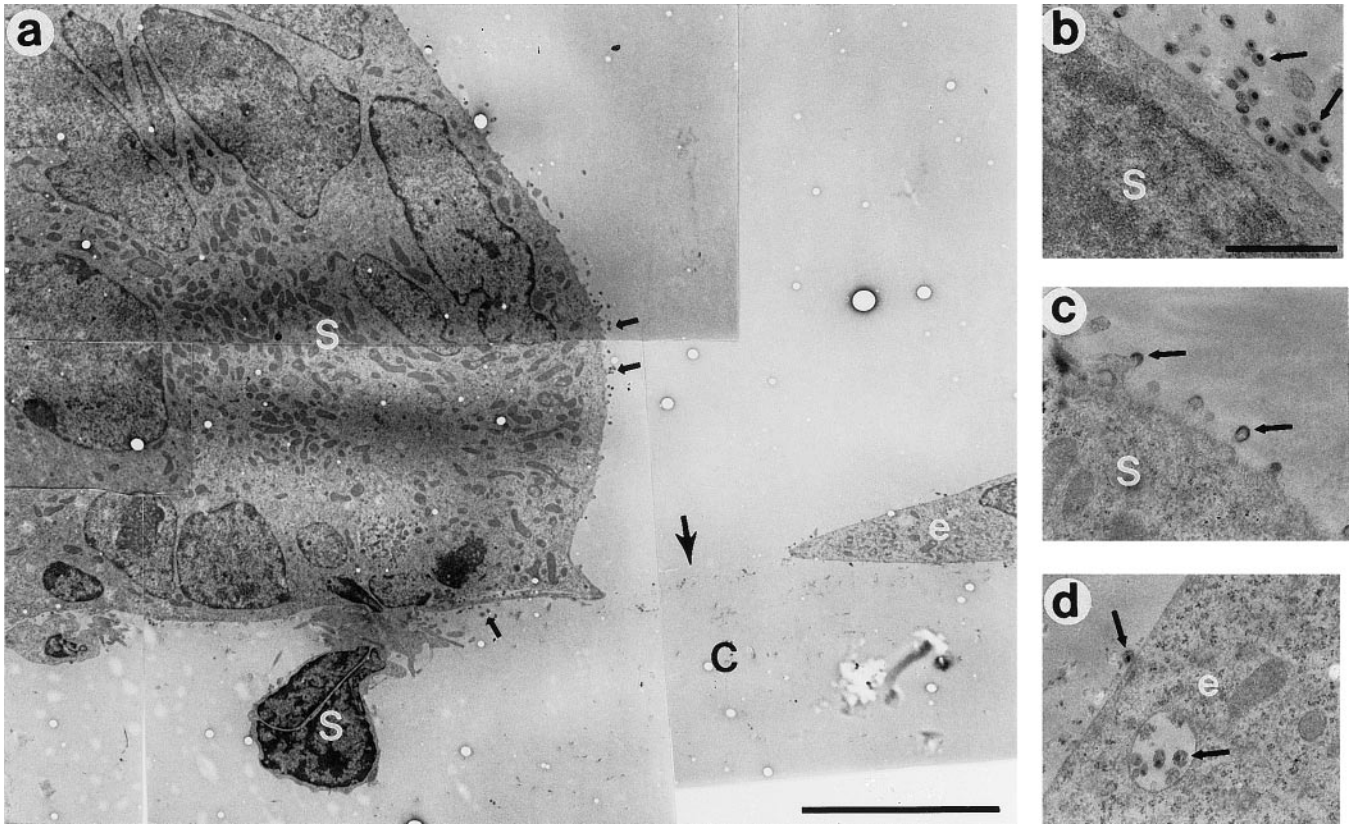

Fig. 8. TEMs of a large syncytium after 96-h incubation atop a bovine aortic endothelial (BAE) monolayer grown to confluency atop a hydrated collagen cushion. (a) A low magnification montage of the portion of the syncytium atop a hole in the endothelial monolayer and the collagen cushion. Representative areas of viral release are noted by small filled arrows. Dorsal surface of syncytium (not shown) exhibited no viral budding. (b) High magnification view of virus (arrows) at the surface of the syncytium. (c) High magnification of budding (arrows) at the surface of the syncytium. (d) High magnification of endothelium with virus adhering (arrow) or in a vesicle (arrow). S, syncytium; C, collagen; e, endothelium. Scale bars: a, 10 μm; b, c, d (in panel b) 1 μm.

Cells that penetrated the monolayer completely could reemerge to the monolayer surface by squeezing through small holes.

A small proportion (10%) of syncytia also translocated on top of endothelial monolayers, but at velocities on average half that on conditioned tissue culture plastic [15]. Small syncytia also penetrated monolayers grown on plastic and could reemerge to the top of the monolayer by squeezing through small holes. To further investigate their invasive properties, syncytia were incubated on BAE monolayers grown to confluency on hydrated collagen gels. This model provided an interesting challenge to syncytia because it allowed them to penetrate the monolayer without having to deal immediately with a plastic barrier and because it reflected a more meaningful representation of blood vessel extravasation. Syncytia seeded on this model initially penetrated the monolayer through tight holes. However, syncytia incubated on this model for longer periods of time (e.g., 12 h or more) invariably generated smooth-edged large holes with diameters equal to or greater than those of the syncytia. Seeding experiments demonstrated that syncytia induced these holes rather than found these holes in the monolayer. TEM analysis demonstrated that, after inducing holes, syncytia penetrated the underlying collagen cushion through complex cellular protrusions, but it was apparent that the syncytium cell body was too large to enter the gel. Syncytia incubated for prolonged periods on this model released virus in a polarized fashion from the surface of the syncytium from which the pseudopod or projection extended through the endothelial hole into the collagen cushion. Virus adhered to and were found in vesicles in the retracting endothelial cells in at least two cases.

The destructive potential of HIV-induced syncytia

HIV-induced SUP-T1 syncytia are capable of invading and disorganizing hydrated collagen and generating large smooth-edged holes in endothelial monolayers. Both of these destructive behaviors are associated with the dynamic extension and retraction of pseudopods and long cylindrical projections with pseudopodial ends. Because motile syncytia form in vivo [D. Shutt, A. Sylwester, J. T. Stapleton et al., unpublished observations], there is the potential for similar destructive behaviors with pathological consequences. Blood vessel wall pathologies [63–66] and the deterioration of lymph node integrity [67, 68] have been demonstrated as features of HIV disease. The destructive behavior of HIV-induced T cell syncytia demonstrated in vitro, therefore, raises the possibility that similar behaviors may be the basis for pathologies in vivo.

ACKNOWLEDGMENTS

The authors are indebted to Seamus Murphy, Dean Abel, and Randy Nessler for technical assistance and to Deb Wessels and

Damon Shutt for help in different aspects of this project, and the W. M. Keck Dynamic Image Analysis Facility at the University of Iowa. This research was funded in part by National Institutes of Health Grants HD18577, AI40040, and DE12161, and a grant from the Carver Trust Foundation.

REFERENCES

1. Bates, P. (1996) Chemokine receptors and HIV-1: an attractive pair. *Cell* **86**, 1–3.
2. Barr'e-Sinoussi, F., Chermann, J. C., Rey, F., Nugeyre, M. T., Chamaret, S., Gruest, J., Daugert, C., Axler, B. C., Vezinet-Brun, F., Rouzioux, C., Rozenbaum, W., Montagnier, L. (1983) Isolation of a T-lymphotropic retrovirus from a patient at risk for acquired immune deficiency syndrome (AIDS). *Science* **220**, 868–871.
3. Popovic, M., Sarngadharan, M. G., Read, E., Gallo, R. C. (1984) Detection, isolation, and continuous production of cytopathic retroviruses (HTLV-111) from patients with AIDS and pre-AIDS. *Science* **224**, 497–500.
4. Levy, J. A., Hoffman, A. D., Kramer, S. M., Landis, J. A., Shimabukuro, J. M., Oshiro, L. S. (1984) Isolation of lymphocytopathic retroviruses from San Fransisco patients with AIDS. *Science* **225**, 840–842.
5. Lifson, J. D., Reyes, G. R., McGrath, M. S., Stein, B. S., Englemann, E. G. (1996) AIDS retrovirus induced cytopathology: Giant cell formation and involvement of CD4 antigen. *Science* **232**, 1123–1127.
6. Rinfret, A., Latendresse, H., Lefebvre, R., St-Louis, G., Jolicoeur, P., Lamarre, L. (1991) Human immunodeficiency virus-infected multinucleated histiocytes in oropharyngeal lymphoid tissues from two asymptomatic patients. *Am. J. Pathol.* **138**, 421–426.
7. Frankel, S., Wenig, B., Burke, A., Mannan, P., Thompson, L., Abbondanzo, S., Nelson, A., Pope, M., Steinman, R. (1996) Replication of HIV-1 in dendritic cell-derived syncytia at the mucosal surface of the adenoid. *Science* **272**, 115–117.
8. Leonard, R., Zagury, D., Disportes, I., Bernard, J., Zagury, J. F., Gallo, . C. (1988) Cytopathic effect of human immunodeficiency virus in T4 cells is linked to the last stage of virus infection. *Proc. Natl. Acad. Sci. USA* **85**, 3570–3574.
9. Kiernan, R., Marshall, J., Bowers R., Doherty, R., McPhee, D. (1990) Kinetics of HIV-1 replication and intracellular accumulation of particles in HTLV-I transformed cells. *AIDS Res. Hum. Retrovir.* **6**, 743–752.
10. Sylwester, A., Shutt, D., Murphy, S., Soll, D. R. (1996) HIV-induced T cell syncytia are self-perpetuating and the primary cause of T cell death in culture. *J. Immun.* **158**, 3996–4007.
11. Soll, D. R. (1997) Researchers in cell motility and the cytoskeleton can play major roles in understanding AIDS. *Cell Motil. Cytoskel.* **37**, 91–97.
12. Sylwester, A., Wessels, D., Anderson, S. A., Warren, R. Q., Shutt, D., Kennedy, R., Soll, D. R. (1993) HIV-Induced syncytia of a T cell line form single giant pseudopods and are motile. *J. Cell Sci.* **106**, 941–953.
13. Shutt, D., Stapleton, J. T., Kennedy, R. C., Soll, D. R. (1995) HIV-induced syncytia in peripheral blood cultures crawl by extending giant pseudopods. *Cell. Immunol.* **166**, 261–274.
14. Soll, D. R., Kennedy R. (1994) The role of T cell motility and cytoskeletal reorganization in HIV-induced syncytium formation: a perspectus. *AIDS Res. Human Retroviruses* **10,** 325–327.
15. Sylwester, A., Shutt, D., Wessels, D., Stapleton, J. T., Stites, J., Kennedy, R. C., Soll, D. R. (1995) T cells and HIV-induced T cell syncytia exhibit the same motility cycle. *J. Leukoc. Biol.* **57**, 643–650.
16. Harada, S. N., Koboyashi, Y., Yamaoto, N. (1987) Clonal selection of human immunodeficiency virus (HIV): serological differences in the envelope antigens of the cloned viruses and HIV prototypes (HTLV-III, LAV, and ARV). *Virol.* **158**, 447–451.
17. Smith, S. D., Shatsky, M., Cohen, P. S., Warake, R., Link, M. P., Glader, B. E. (1984) Monoclonal antibody and enzymatic profiles of human-malignant T-lymphoid cells and derived cell lines. *Cancer Res.* **44**, 5657–5660.
18. Soll, D. R. (1995) The use of computers in understanding how cells crawl. *Int. Rev. Cytol.* **163**, 43–104.
19. Soll, D. R., Voss, E., Varnum-Finney, B., Wessels, D. (1988) The ''Dynamic Morphology System'': a method for quantitating changes in shape, pseudopod formation and motion in normal mutant amoebae of *Dictyostelium discoideum*. *J. Cell. Biochem.* **37**, 177–192.
20. Soll, D. R. (1988) 'DMS', a computer-assisted system for quantitating motility, the dynamics of cytoplasmic flow and pseudopod formation: its application to *Dictyostelium chemotaxis*. In *Optical Approaches to the Dynamics of Cellular Motility* (J. Condeelis, ed.) Supplement to *Cell Motil. Cytoskel.* **10**, 91–106.
21. Murphy, S., Sylwester, A., Kennedy, R. C., Soll, D. R. (1995) Phagocytosis of individual $CD4^+$ T cells by HIV-induced T cell syncytia. *AIDS Res. Human Retroviruses* **11**, 433–441.
22. Sylwester, A. (1996) *The in vitro biology of HIV-induced T cell syncytia*. Ph.D. Thesis, Iowa City: University of Iowa.
23. Parrott, D. V., Wilkinson, P. C. (1981) Lymphocyte locomotion and migration. *Prog. Allergy* **28**, 193–284.
24. Mackay, C. R. (1992) Migration pathways and immunologic memory among T lymphocytes [Review]. *Semin. Immunol* **4**, 51–58.
25. McEver, R. P. (1992) Leukocyte-endothelial cell interactions [Review]. *Curr. Op. Cell. Biol.* **4**, 840–849.
26. Butcher, E. C. (1993) Specificity of leukocyte-endothelial interactions and diapedesis: physiologic and therapeutic implication of an active decision process. [Review]. *Res. Immunol.* **144**, 695–698.
27. Granger, D. N., Kubes, P. (1994) The microcirculation and inflammation: modulation of leukocyte-endothelial cell adhesion [Review]. *J. Leukoc. Biol.* **55**, 662–675.
28. Budka, H. (1986) Multinucleated giant cells in brain; a hallmark of the acquired immune deficiency syndrome (AIDS) [Review]. *Acta Neuropathol.* **69**, 253–258.
29. Gray, F., Fenelon, G. Gherardi, R., Favolini, M., Goulon, M., Guillard, A., Poirier, J. (1988) Neuropathological study of 15 cases of AIDS with multinucleated giant cell encephalitis of AIDS. *Ann. Pathol.* **8**, 281–289.
30. Michaels, J., Price, R. W., Rosenblum, M. K. (1988) Microglia in the giant cell encephalitis of AIDS: Proliferation, infection and fushion. *Acta Neuropathol.* **76**, 373–379.
31. Li, Y. Y., Cheung, H. T. (1992) Basement membrane and its components on lymphocyte adhesion, migration, and proliferation. *J. Immunol.* **149**, 3174–3181.
32. Allen, T. D., Schor, S. L., Schor, A. M. (1984) An ultrastructure review of collagen gels. A Model system of cell-matrix, cell-basement membrane, and cell-cell interactions. *Scanning Electron. Microsc.* **1**, 375–390.
33. Gospodarowicz, D., Moran, J., Braun, D., Birdwell, C. (1979) Clonal growth of bovine endothelial cell: fibroblast growth factor as a survival agent. *Proc. Natl. Acad. Sci. USA* **73**, 4120–4214.
34. Vlodavsky, I., Gospodarowicz, D. (1979) Structural and functional alterations in the surface of vascular endothelial cells associated with the formation of a confluent cell monolayer and with the withdrawal of fibroblast growth factor. *J. Supramol. Struct.* **12**, 73–114.
35. Vlodoavsky, I., Lui, G. M., Gospodarowicz, D. (1980) Morphological appearance, growth behavior and migratory activity of human tumor cells maintained on extracellular matrix versus plastic. *Cell* **19**, 607–616.
36. Gospodarowicz, D., Delgado, D., Vlodavsky, I. (1980) Permissive effect of the extracellular matrix on cell proliferation in vitro. *Proc. Natl. Acad. Sci. USA* **77**, 4094–4098.
37. Matzner, Y., Vlodavsky, I., Michaeli, R. I., Eldor, A. A. (1990) Selective inhibition of neutrophil activation by the subendothelial extracellular matrix: Possible role in protection of the vessel wall during diapedesis. *Exp. Cell Res.* **189**, 233–240.
38. De Bono, D. (1976) Endothelial-lymphocyte interactions in vitro. *Cell Immunol.* **26**, 78–88.
39. Delvos, U., Gajdusek, C., Sage, H., Harker, L. A., Schwartz, S. M. (1982) Interactions of vascular wall cells with collagen gels. *Lab. Invest.* **46**, 61–72.
40. Cavender, D. E., Cearns-Spielman, J., Brrus, C. Q., Dunaway-Piccioni, D. (1991) T-cell adhesion to extracellular matrix molecules secreted by endothelial cells cultured on a substrate of type IV collagen. *J. Immunol. Meth.* **14**, 185–196.
41. Haston, W., Shields, J., Wilkinson, P. (1982) Lymphocyte locomotion and attachment on two-dimensional surfaces and in three-dimensional matrices. *J. Cell. Biol.* **92**, 747–752.
42. Sundqvist, K., Otteskog, P. (1986) Anchorage and lymphocyte function: collagen and the maintenance of motile shape in T cells. *Immunol.* **58**, 365–369.
43. Arencibia, L., Sundqvist, K. (1989) Collagen receptor on T lymphocytes and the control of lymphocyte motility. *Eur. J. Immunol.* **19**, 929–934.
44. Dang, H., Torimoto, Y., Schlossman, S., Morimoto, C. (1990) Human CD4 helper T cell activation: Functional involvement of two distinct collagen receptors, 1F7 and VLA integrin family. *J. Exp. Med.* **172**, 649–652.
45. Van De Wielvan, K., Van Kooyk, E., De Boer, A., Huijbens, F., Weder, P., Van De Kasttele, W., Melief, C., Figdor, C. (1992) Adhesion of T and B lymphocytes to extracellular matrix and endothelial cells can be regulated through the β subunit of VLA. *J. Cell Biol.* **117**, 461–470.
46. Sundqvist, K. G., Havzenberger, D., Hultenby, K., Bergsrom, S. E. (1993) T lymphocyte infiltration of two and three-dimensional collagen substrate by an adhesive mechanism. *Exp. Cell. Res.* **206**, 100–110.
47. Savion, N., Vlodavsky, I., Fuks, J. (1984) Interaction of T lymphocytes and macrophages with cultured vascular endothelial cells: attachment, inva-

sion, and subsequent degradation of the subendothelial extracellular matrix. *J. Cell Physiol.* **118**, 169–178.
48. Kammer, G., Sapolsky, A., Malemud, C. (1985) Secretion of an articular cartilage proteoglycan-degrading enzyme activity by murine T lymphocytes in vitro. *J. Clin. Invest.* **76**, 395.
49. Kramer, M., Bininger, L., Schirrmacher, V., Moll, H., Prester, M., Nerz, G., Simon, M. (1986) Characterization and isolation of a trypsin-like serine protease from a long-term culture cytolytic T cell line and its expression by functionally distinct T cells. *J. Immunol.* **136**, 4644.
50. Simon, M. M., Simon, H. G., Fruth, U., Epplen, J., Mueller-Hermelink, H. K., Kramer, M. D. (1987) Cloned cytolytic T-effector cells and their malignant variants produce an extracellular matrix degrading trypsin-like serine proteinase. *Immunol.* **60**, 219–230.
51. Vlodavsky, I., Schirrmacher, V., Ariav, Y., Fuks, Z. (1983) Lymphoma cell interaction with cultured vascular endothelial cells and with the subendothelial basal lamina: attachment, invasion and morphological appearance. *Invasion Metastasis* **3**, 81–97.
52. Bender, J. R., Pardi, R., Kosek, J., Engleman, E. G. (1989) Evidence that cytotoxic lymphocytes alter and traverse allogeneic endothelial cell monolayers. *Transplant.* **47**, 1047–1053.
53. Sanderson, C. J., Glauert, A. M. (1979) The mechanism of T-cell-mediated cytotoxicity. VI. T cell projections and their role in target cell killing. *Immunol.* **36**, 119–129.
54. Condeelis, J. (1993) Life at the leading edge: the formation of cell protrusions. *Annu. Rev. Cell Biol.* **9**, 411–444.
55. Shimizu, Y., Newman, W., Gopal, T. V., Horgan, K. J., Graber, N., Beal, L. D. (1991) Four molecular pathways of T cell adhesion to endothelial cells: Roles of LFA-1, VCAM-1, and ELAM-1 and changes in pathway hierarchy under different activation conditions. *J. Cell. Biol.* **113**, 1203–1212.
56. Picker, L. J. (1992) Mechanisms of lymphocyte homing [Review]. *Curr. Op. Immunol.* **4**, 277–286.
57. DeBruyn, P. P. H., Michelson, S., Thomas, T. B. (1971) The migration of blood cells of the bone marrow through the sinusoidal wall. *J. Morph.* **133**, 47–38.
58. Anderson, A. O., Anderson, D. (1976) Lymphocyte emigration from high endothelial venules in rat lymph nodes. *Immunol.* **31**, 731–748.
59. Vandendriessche, T., Verschueren, H., Verhaegen, S., Van Hecke, D., DeBaetselier, P. (1991) Experimental analysis of the metastatic phenotype of malignant leukocytes [Review]. *Anticancer Res.* **11**, 49–74.
60. Cho, Y., DeBruyn, P. P. H. (1981) Transcellular migration of lymphocytes through the walls of the smooth-surfaces squamous endothelial venules in the lymph node: Evidence for the direct entry of lymphocytes into the blood circulation of the lymph node. *J. Ultrastruct. Res.* **74**, 259.
61. Dingemans, K. P., Roos, E., Vander Bergh Weerman, M. A., Van De Pavert, I. V. (1978) Invasion of liver tissue by tumor cells and leukocytes: comparative ultrastructure. *J. Natl. Cancer Inst.* **60**, 583–598.
62. Doukas, J., Shepro, D., Hechtman, H. B. (1987) Vasoactive amines directly modify endothelial cells to affect polymorphonuclear leukocyte diapedesis in vitro. *Blood* **69**, 1563–1569.
63. Dickson, D. W., Belman, A. L., Park, Y. D., Wiley, C. Horoupian, D. S., Llena, J., Kure, K., Lyman, W. D., Morecki, R., et al. (1989) Central nervous system pathology in pediatric AIDS: An autopsy study. *APMIS (Suppl.)* **97**, 40.
64. Lackner, A. A. (1994) Pathology of simian immunodeficiency virus induced disease, p. 35-64. In *Simian Immunodeficiency Virus* (N. L. Letvin and R. C. Desrosiers, ed.), New York: Springer-Verlag.
65. Chalifoux, L. V., Simon, M. A., Pauley, D. R., Mackey, J. J., Wyand, M.S., Ringler, D. J. (1992) Arteriopathy in macaques infected with SIV virus. *Lab. Invest.* **67**, 338–349.
66. Rhodes, R. H. (1991) Evidence of serum-protein leakage across the blood-brain barrier in AIDS. *J. Neuropathol. Exp. Neurol.* **50**, 171–183.
67. Pantaleo, G., Graziosi, C., Fauci, A. S. (1993) The role of lymphoid organs in the pathogenesis of HIV infection [Review]. *Semin. Immunol.* **5**, 157–163.
68. Fauci, A. S. (1993) Multifactorial nature of human immunodeficiency virus disease: Implications for therapy [Review]. *Science* **262**, 1011–1018.